Monthly Notices of the ROYAL ASTRONOMICAL SOCIETY
MNRAS **457,** 2–8 (2016) doi:10.1093/mnras/stv2846

Discovery of a Fanaroff–Riley type 0 radio galaxy emitting at γ-ray energies

Paola Grandi,[1]★ Alessandro Capetti[2]★ and Ranieri D. Baldi[1,3]★

[1]*INAF-IASFBO, Via Gobetti 101, I-40129 Bologna, Italy*
[2]*INAF-Osservatorio Astrofisico di Torino, Strada Osservatorio 20, I-10025, Pino Torinese, Italy*
[3]*Department of Physics and Astronomy, The University, Southampton SO17 1BJ, UK*

Accepted 2015 December 2. Received 2015 November 30; in original form 2015 August 31

ABSTRACT

We present supporting evidence for the first association of a *Fermi* source, 3FGLJ1330.0−3818, Acero et al. (2015) with the Fanaroff–Riley type 0 (FR 0) radio galaxy Tol1326−379. FR 0s represent the majority of the local population of radio-loud active galactic nuclei but their nature is still unclear. They share the same nuclear and host properties as FR Is, but they show a large deficit of extended radio emission. Here we show that FR 0s can emit photons at very high energies. Tol1326−379 has a GeV luminosity of $L_{>1\,\mathrm{GeV}} \sim 2 \times 10^{42}$ erg s^{-1}, typical of FR Is, but with a steeper γ-ray spectrum ($\Gamma = 2.78 \pm 0.14$). This could be related to the intrinsic jet properties but also to a different viewing angle.

Key words: galaxies: active – galaxies: individual: Tol1326−379 – galaxies: jets – gamma-rays: galaxies – radio continuum: galaxies.

1 INTRODUCTION

Radio galaxies (RGs) have been historically divided into faint edge-darkened Fanaroff–Riley type I (FR I) and bright edge-brightened FR II galaxies (Fanaroff & Riley 1974) based on their extended radio morphology with the transition occurring at, approximately, a radio power of $P_{178\,\mathrm{MHz}} \sim 10^{25}$ W Hz^{-1} sr^{-1}. From the optical point of view, RGs are split into broad-line radio galaxies (BLRGs) and narrow-line RGs. The latter can be further classified as high-excitation galaxies and low-excitation galaxies (LEGs) based on their optical emission-line ratios (Buttiglione et al. 2010). While high-excitation galaxies and BLRGs show almost exclusively a FR II morphology, LEGs can assume either radio morphology. It is believed that in LEGs, the luminosity of the active galactic nucleus (AGN) is sustained by hot gas via advection-dominated flow-like/Bondi accretion (Balmaverde, Baldi & Capetti 2008), while in BLRGs and high-excitation galaxies by a cold geometrically thin and optically thick disc (Best & Heckman 2012; Heckman & Best 2014). Steep-spectrum radio quasars (SSRQs) are similar to BLRGs but more distant and luminous. FR Is and FR IIs are considered the parent population of BL LACs and flat-spectrum radio quasars (FSRQs), respectively (Urry & Padovani 1995).

Being observed at large angles, the jets of RGs and SSRQs (collectively named misaligned AGNs or MAGNs) do not benefit from the strong Doppler amplification typical of blazars. Although geometrically disfavoured (i.e. less amplified), RGs and SSRQs have been detected above 100 MeV. The *Fermi* satellite found 11 MAGNs in only 15 months of the Large Area Telescope (LAT) survey (Abdo et al. 2010c), with four of them also detected in the TeV band. Although their number is a tiny fraction of the total *Fermi* detected sources, their discovery had a strong impact on the study of the high-energy process in AGNs.

A clear link, in at least two BLRGs, 3C 111 and 3C 120, has been established between the expulsion of bright superluminal knots from the radio core and intense γ-ray flares (Grandi, Torresi & Stanghellini 2012; Casadio et al. 2015).

The firm detection of GeV emission from the radio lobes in nearby RG Centaurus A has shown that extranuclear extended regions can be a source of γ-ray photons, implying the presence of highly energetic particles at large distances from the nucleus (Abdo et al. 2010b). Because their radiative lifetimes (<1 to 10 million yr) approach plausible electron transport time-scales across the lobes, their presence is difficult to explain unless successive particle acceleration occurs even at large distances from the black hole.

Spectral energy distribution (SED) studies of FR I RGs show that a pure one-zone homogeneous, synchrotron self-Compton emitting region is inadequate in reproducing the radio to TeV data, stimulating the elaboration of more complex models. Stratified jets with different regions interacting with each other (Georganopoulos & Kazanas 2003; Ghisellini, Tavecchio & Chiaberge 2005; Böttcher & Dermer 2010) as well as magnetic reconnection events along the jet (Giannios, Uzdensky & Begelman 2010) or in the vicinity of the black hole (Khiali, de Gouveia Dal Pino & Sol 2015) have been suggested as possible sources of γ-ray photons. Hadronic models based on proton–photon interaction (for

★E-mail: grandi@iasfbo.inaf.it (PG); capetti@oato.inaf.it (AC); r.baldi@soton.ac.uk (RDB)

a review, see Böttcher 2012) have also been explored for providing possible connections among AGNs, ultra-high-energy cosmic rays and neutrinos (Becker & Biermann 2009).

All these results are based on the study of the brightest MAGNs discovered in the first years of the *Fermi*-LAT activity, i.e. bright radio sources with a flux density of 2 Jy or more. The recent publication of the new *Fermi*-LAT point-source catalogue (3FGL) (Acero et al. 2015) and the *Fermi*-LAT AGN catalogues (3LAC) (Ackermann et al. 2015) with 4 yr of data now allow us to extend the study of GeV RGs to lower fluxes. Although the standard picture, i.e. the predominance of bright FR Is among MAGNs, is confirmed, we can now enter into the unexplored territory of fainter radio AGNs. Indeed, we propose here the first association between a 3LAC γ-ray source and a FR 0 galaxy.

The cross-matching of radio and optical data favoured by the advent of large area surveys has surprisingly revealed that the bulk of the RG population lacks prominent extended radio structures. Best & Heckman (2012) built a sample of RGs by cross-correlating the Sloan Digital Sky Survey (SDSS), the National Radio Astronomy Observatory (NRAO) Very Large Array Sky Survey (NVSS), and the Faint Images of the Radio Sky at Twenty centimetres (FIRST) survey data sets. This sample is selected at $F_{1.4} > 5$ mJy and it includes RGs up to $z \sim 0.3$, covering the range $L_{1.4} \sim 10^{22}$–10^{26} W Hz^{-1}. Most of them (∼80 per cent) are unresolved or barely resolved at the 5-arcsec FIRST resolution, corresponding to a limit to their size of ∼10 kpc (Baldi & Capetti 2009). The lack of extended radio structures, which characterize the morphology of the traditional Fanaroff–Riley classes (FR I and FR II), suggests defining these objects as FR 0s (see Baldi, Capetti & Giovannini 2015b).

FR 0s share the same nuclear and host properties as FR Is. By comparing FR Is and FR 0s of similar AGN power, estimated from the optical line luminosity, FR 0s show the same radio core power but a strong deficit of extended radio emission. Most of them (∼70 per cent) can be classified as LEGs, the same spectroscopic class to which FR Is belong. Finally, the hosts of these two classes are effectively indistinguishable, being in both cases red early-type galaxies with central black hole masses larger than $\sim 10^8$ M$_\odot$ (Baldi & Capetti 2009, 2010; Sadler et al. 2014; Baldi, Capetti & Giovannini 2015a).

Although FR 0s represent the majority of the low-luminosity RGs in the local Universe, they are a puzzling class of AGNs, completely unexplored at high energies.

In this paper, we show that the galaxy Tol1326−379, identified as the counterpart of the γ-ray source 3FGLJ1330.0−3818 and classified in the 3LAC as a FSRQ, was actually the first FR 0 radio source discovered in the GeV sky.

A cosmology with $H_0 = 67$ km s^{-1} Mpc^{-1}, $\Omega_m = 0.32$ and $\Omega_\Lambda = 0.68$ is assumed.

2 3FGLJ1330.0−3818 AND TOL1326−379

The γ-ray source 3FGLJ1330.0−3818 was detected by *Fermi* with a significance of $\sim 5\sigma$, a flux above 1 GeV of $F_{>1\,\mathrm{GeV}} = (3.1 \pm 0.8) \times 10^{-10}$ phot cm^{-2} s^{-1} and a power-law index $\Gamma = 2.78 \pm 0.14$ (Acero et al. 2015).

3FGLJ1330.0−3818 is listed in the 3LAC catalogue. It is associated with the early-type galaxy Tol1326−379 at $z = 0.028\,43$ with a Bayesian probability of association of 90 per cent. The Bayesian method calculates the posterior probability that a source from a catalogue of candidates is the counterpart of a γ-ray source detected by the LAT, evaluating the significance of a spatial coincidence between the candidate counterpart and the LAT-detected source. For more details, see Abdo et al. (2010a).

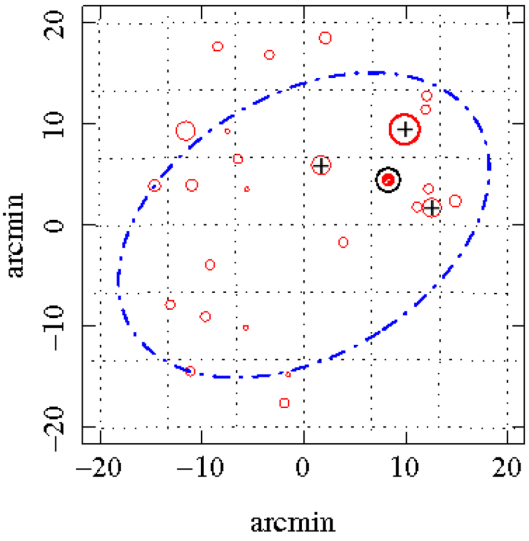

Figure 1. NVSS radio sources in the field of 3FGLJ1330.0−−818. Symbol sizes are proportional to the flux density at 1.4 Hz. Tol1326−379 is marked with the red point. Three bright radio sources, NVSS J132911−380918, NVSS J132952−381251 and NVSS J132857−381703 (cross symbols) are within the Fermi position error ellipse, but they are rejected as possible counterparts (see text). This image was produced using the ASDC tool http://www.asdc.asi.it/fermi3fgl/.

To strengthen the association proposed by the 3LAC catalogue, we explored the region around 3FGLJ1330.0−3818 within the 95 per cent γ-ray position error ellipse (20 × 13 arcmin) looking for alternative identifications. We considered all radio sources with a NVSS flux density larger than 20 mJy (∼3 times fainter than Tol1326−379), finding three objects spanning the range 70 to 240 mJy (see Fig. 1). Their radio spectral indices, estimated between 0.843 and 1.4 GHz, are steep ($\alpha_r \sim 0.7$–0.9) and none of them is detected at 4.8 GHz with the PARKES telescope (Griffith & Wright 1993), implying that their flux densities are less than ∼35 mJy, suggesting the dominance of the extended radio emission. Furthermore, none of them has a Two Micron All Sky Survey (2MASS) counterpart apart from Tol1326−379, which shows an early-type morphology. This confirms that Tol1326−379 is the most likely association.

3 THE GALAXY TOL1326−379

3.1 Optical properties

The optical spectrum of Tol1326−379 from the 6dF Galaxy Survey (6dFGS) (Jones et al. 2004, 2009) is presented in Fig. 2, left-hand panel. It does not show any evidence for broad emission lines, arguing against its identification as a FSRQ; on the other hand, the equivalent width (EW) of the emission lines largely exceeds the limit of 5 Å commonly adopted for BL Lac objects (Stickel et al. 1991). We obtained, in particular, EW(H α) ∼45 ± 4 Å and EW([O III]) ∼8 ± 1 Å. The diagnostic line ratios ($\log$[O III]/H$\beta = 0.10$, $\log$[N II]/H$\alpha = -0.03$, $\log$[O I]/H$\alpha = -0.40$ and $\log$[S II]/H$\alpha = 0.01$) are characteristic of a LEG spectrum (Kewley et al. 2006; Buttiglione et al. 2010). This lends further weight against its association with a FSRQ, because such sources always show a high-ionization optical spectrum (Shaw et al. 2012).

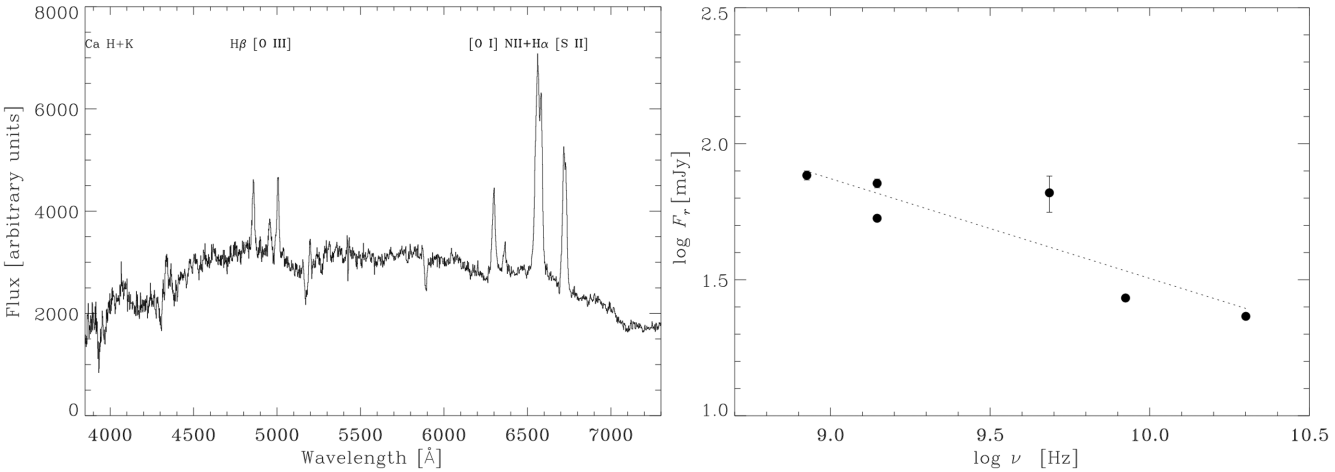

Figure 2. Left: Optical spectrum of Tol1326−379 from the 6dF Galaxy Survey (Jones et al. 2004). Right: Radio spectrum of Tol1326−379. Data are from the literature (Wright et al. 1994; Condon et al. 1998; Mauch et al. 2003; Healey et al. 2007; Feain et al. 2009). The 20-GHz flux density was measured with the Australian Telescope Compact Array (see text for details). The dotted line is the single power fit to the data having a slope of 0.37.

Unfortunately, the 6dFGS spectrum is not flux calibrated. To obtain the emission-line luminosity, we need to rely on an indirect estimate. We derived the flux in the *J*-band 2MASS image from a synthetic aperture of 6.7 arcsec, the diameter of the 6dFGS fibre, after having degraded the image resolution to match the seeing reported in the observing log. We then adopted a $V - J$ colour of 2.43 (Mannucci et al. 2001), typical of early-type galaxies, and obtained a magnitude of $V = 15.1$. From its measured EW, we finally obtain an [O III] flux of 3.2×10^{-15} erg cm^{-2} s^{-1} and a luminosity of 4×10^{40} erg s^{-1}.

To assess the accuracy of this procedure, we performed the same analysis on a group of seven early-type emission-line galaxies in common between the 6dFGS and the SDSS survey. Our line measurements agree with those provided by the SDSS data base within a factor of 4.

From its 2MASS image, we derived a total *K* magnitude of 11.22, corresponding to a luminosity of 1.0×10^{11} solar luminosity. The tight correlation between $M_{\rm BH}$ and the near-infrared bulge luminosity proposed by Marconi & Hunt (2003) allows us to estimate (within a factor of 2) the black hole mass of $M_{\rm BH} = 2 \times 10^8$ M$_\odot$.

Using the relation $L_{\rm bol} = 3500 L_{[\rm O\,III]}$ measured by Heckman et al. (2004), we obtain a bolometric luminosity $L_{\rm bol} = 44.1$ erg s^{-1} (with an uncertainty of 0.4 dex) for this source. The Eddington-scaled accretion rate of Tol1326−379 is $\dot{L} = L_{\rm bol}/L_{\rm Edd} \sim 5 \times 10^{-3}$, a value typical of LEGs (Best & Heckman 2012).

3.2 Radio properties

We collected the radio flux density data from the NASA/IPAC Infrared Science Archive and Extragalactic Database (NED). To these data we added our own measurement at 20 GHz from the Australian Telescope Compact Array (ATCA); the observations were obtained on 2004 October 27 (project C1049, principal investigator Ekers) as part of the AT20G survey (Murphy et al. 2010), centred at 19.9 GHz, with a bandwidth of 256 MHz and duration of 3.6 min. We used PKS 1934−638 for the primary flux calibration, 1036−52 as the bandpass calibrator and PKS 1349−439 as the phase calibrator. After deconvolution, the source appears as unresolved (angular resolution of 10 arcsec); we perform a Gaussian fit using the JMFIT task of the AIPS software[1] to estimate its flux density of 23.2 ± 0.8 mJy. The available radio data cover the frequency range from 843 MHz to 20 GHz (see Fig. 2, right-hand panel). None of the available radio images shows extended emission and in particular Tol1326−379 is reported by Healey et al. (2007) to be a point source in their CRATES catalogue at 8.4 GHz. The angular resolution provided by the ATCA observation is ∼2 arcsec. The overall spectral slope is $\alpha = 0.37$ but the data points show a large scatter. This is, in part, due to the source variability; indeed, its flux density varied from 53.2 to 71.5 mJy in the NVSS and ATCA observations, respectively, two measurements obtained at the same frequency and with similar spatial resolution. In addition, the observations have rather different spatial resolution, typically ∼45 arcsec for the four lower frequencies and of a few arcsecs for the data at 8.4 and 20 GHz. The radio spectrum measured between these two high-frequency (and high-resolution) measurements is even flatter than the overall value, $\alpha_{8.4\text{–}20\,GHz} = 0.11$. The core dominance parameter *R*, defined as the ratio between the 4.85 and 1.4 GHz flux densities, is $\log R = -0.03$.

Summarizing, Tol1326−379 fulfils all the spectro-photometric requirements for a FR 0 classification listed by Baldi et al. (2015a). It is an early-type galaxy with a black hole mass larger than 10^8 M$_\odot$, a low-excitation optical spectrum and a high radio core dominance. Furthermore, Tol1326−379, given its radio luminosity at 1.4 GHz of 2×10^{39} erg s^{-1}, falls within the region typical of FR 0s in the diagram shown in Fig. 3, which compares the total radio and emission-line luminosities. It also shows, as a characteristic of this class of sources, a large deficit (a factor of ∼300) of radio emission with respect to FR I RGs with equal emission-line power. Tol1326−379 is also consistent, considering the relatively large errors related to the line measurement, with the core–[O III] luminosity relation found for FR Is (Baldi et al. 2015a), another crucial prerogative of FR 0s.

3.3 γ-ray properties

We explored the position of Tol1326−379 in a plot where the radio luminosities at 1.4 GHz of all the blazars and MAGNs of the clean

[1] The NRAO Astronomical Image Processing System (AIPS) is a package that supports the reduction and analysis of data taken with radio telescopes.

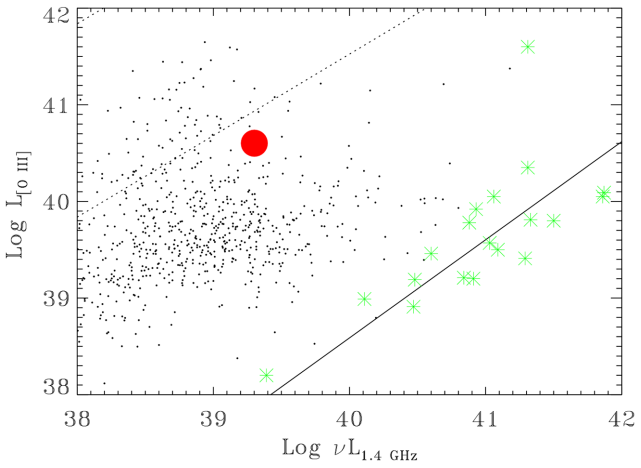

Figure 3. Logarithm of the radio versus [O III] luminosities (both in erg s^{-1}) for the SDSS/NVSS sub-sample ($0.03 < z < 0.1$) analysed by Baldi & Capetti (2009) and mainly composed of FR 0 sources. The solid line reproduces the line–radio correlation followed by FR Is of the 3CR sample (green stars). The dashed line marks the boundary of the location of Seyfert galaxies (e.g. Whittle 1985). FR 0s show a strong deficit of total radio emission, occupying the region to the left of the FR Is (Baldi et al. 2015a). Tol1326−379 (red point) falls into the FR 0 area.

3LAC sample (with known optical classification and red shift) are reported as a function of the γ-ray luminosities (see Fig. 4, left-hand panel). We also add 3C 111 and Cen B (not found in the clean sample because of their low Galactic latitudes) and 3C 120, which is in the 15-month sample of MAGNs and has recently had strong flares (Casadio et al. 2015). As the origin (jet or lobes) of the γ-ray emission from Fornax A is unclear, we prefer not to include it.

We derived for all sources in the 3LAC catalogue the k-corrected 1.4-GHz rest-frame flux density by assuming $\alpha_r = 0$ for blazars and 0.8 for MAGNs.[2] For Tol1326−379, we assume the observed value of $\alpha_r = 0.37$. As expected, different classes lie in different zones of the diagram with FSRQs at higher luminosities than BL Lacs. We recover the well-known radio versus γ-ray correlation for blazars (Ghirlanda et al. 2010; Ackermann et al. 2011). On average, MAGNs are offset from the blazar strip showing a radio excess with respect to BL Lacs and FSRQs with similar γ-ray luminosities. This is due to the additional contribution from extranuclear radio emission. Tol1326−379 falls into the low-luminosity tail of the blazar strip. It is, together with Inverse Compton (IC) 310, the least powerful RG with γ-ray detection.

To explore the nature of our source further, the γ-ray spectral slope (Γ) of blazars and MAGNs of the clean 3LAC sample was plotted in Fig. 4, right-hand panel, as a function of the rest-frame isotropic luminosity above 1 GeV ($L_{>1\,\mathrm{GeV}}$ in erg cm^{-1} s^{-1}). As is well known, different classes of AGNs occupy different locations in the Γ versus $L_{>1\,\mathrm{GeV}}$ plane (Abdo et al. 2010c). FSRQs and SSRQs are in the upper right part of the diagram (high luminosities and steep spectra), BL Lacs in the bottom right side (low luminosities and flat spectra), while RGs are all at low luminosities, but with a large scatter in spectral indices. It is evident that Tol1326−379 falls into the general RG area and not into the FSRQ region.

[2] In some cases, the 3LAC radio flux density was provided at different radio frequencies (for example, at 20 GHz or at 843 MHz). The above reported spectral radio slopes were also adopted to convert the listed flux to the 1.4-GHz flux.

4 DISCUSSION

The 3LAC catalogue associates the γ-ray source 3FGLJ1330.0−3818 with the galaxy Tol1326−379. We confirm that no other flat radio source brighter than Tol1326−379 at 5 GHz is present within the 95 per cent error circle position of 3FGLJ1330.0−3818. Although flat in the radio, Tol1326−379 is not a FSRQ but a FR 0 RG, the first source of this new radio class with a γ-ray counterpart.

Several observations support this conclusion:

(i) Tol1326−379 is an early-type galaxy at $z = 0.028\,43$.

(ii) It does not show any evidence for broad emission lines, arguing against its identification as an FSRQ.

(iii) The high values of the line equivalent widths exclude the possibility that it is a BL Lac.

(iv) Its line ratios are typical of LEGs.

(v) Its estimated black hole mass of $M_{BH} = 2 \times 10^8$ $M_\odot$ and accretion rate $\dot{L} = L_{bol}/L_{Edd} \sim 5 \times 10^{-3}$ are characteristic of a radio-loud AGN (Chiaberge & Marconi 2011) associated with low-efficiency accretion flows.

(vi) It is unresolved in the radio images, showing a high core dominance and a flat radio spectrum.

(vii) In a radio versus [O III] luminosity plot, it falls into the FR 0 region and not in the FR I area.

In Fig. 5, we present the SED of Tol1326−379. Besides the radio and Fermi observations already discussed, we complement them with *WISE*, *Galex* and *ROSAT* data.

Tol1326−379 is detected at high significance by the *WISE* satellite in all four bands and its colours are $W1 - W2 = 0.38 \pm 0.03$ and $W2 - W3 = 2.58 \pm 0.03$, respectively. These are significantly different from those typical of elliptical galaxies (Wright et al. 2010). This indicates that the emission seen, at least in the $W3$ band, is dominated by the AGN component. Indeed, Tol1326−379 lies in a region populated by BL Lac objects (Massaro et al. 2011), although offset from the main blazar strip.

The ultraviolet (UV) data, from the *Galex* archive,[3] are corrected for galactic extinction assuming $E(B - V) = 0.0678$. In the X-ray band, Tol1326−379 was only detected by the PSPC instrument (0.1–2.4 keV) on board the *ROSAT* satellite. Its count rate reported in the ROSAT All-Sky Survey Faint Source Catalogue[4] is 0.029 ± 0.013 c s^{-1}. This can be converted to an unabsorbed flux of $F_{0.1\text{–}2.4\,\mathrm{keV}} = (7.6 \pm 3.4) \times 10^{-13}$ erg s^{-1} cm^{-2} if a power law with spectral slope $\Gamma_x = 2$ and Galactic absorption of $N_H = 5.5 \times 10^{20}$ cm^{-2} are assumed. Due to the low spatial resolution of the UV and X-ray images, and the lack of any spectral information, the corresponding measurements should be considered as upper limits, as they include the host galaxy emission. In particular, its soft X-ray luminosity is compatible with that expected from the hot corona of an early-type galaxy with the luminosity estimated above for our source (Fabbiano, Kim & Trinchieri 1992).

The SED of Tol1326−379 is compared to those of Centaurus A and M87, the prototype nearby FR I RGs. Despite the similar radio luminosity, M87 is less luminous than Tol1326−379 by a factor of 30 at 1 GeV and has a flat SED in the γ-ray domain. In contrast, Centaurus A and Tol1326−379 are quite similar in shape but the former source is about two orders of magnitude fainter.

Balmaverde & Capetti (2006) found that the SEDs of FR I nuclei differ from those of BL Lacs. This is partly related to the frequency

[3] http://galex.stsci.edu/GR6/

[4] http://www.xray.mpe.mpg.de/rosat/survey/rass-fsc/

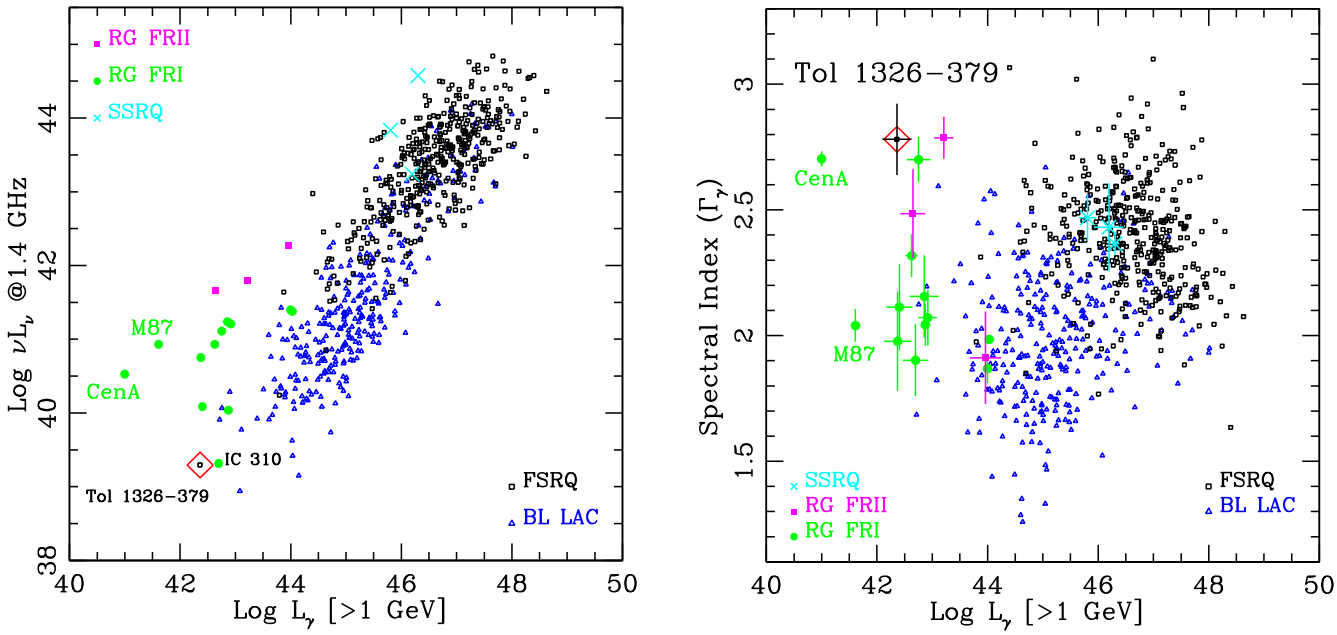

Figure 4. Left: Radio luminosity of the 3LAC FR I RGs (green circles), FR II radio sources (magenta squares), BL Lacs (open blue triangles), FSRQs (open black squares) and SSRQs (cyan crosses) is plotted as a function of the γ-ray luminosity between 1 and 100 GeV. MAGNs, extended at 1.4 GHz, are more luminous in radio than blazars with similar γ-ray luminosity. Tol1326−379 (red open diamond) has a typical FR I γ-ray luminosity but falls into the low-luminosity tail of the blazar strip. Right: γ-ray spectral slope versus 1–100 GeV luminosity. Tol1326−379 is located in the MAGN region and outside the FSRQ zone. For clarity, error bars are reported for non-blazars only. All the luminosities are in erg s^{-1}.

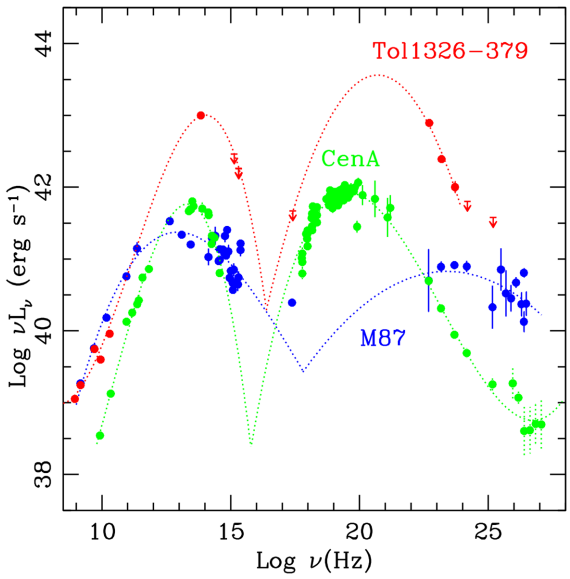

Figure 5. SEDs of Tol1326−379 (red symbols) compared to those of Cen A (green) and M87 (blue). The dotted lines are polynomial functions connecting the points and do not represent model fits to data. Data are collected from the literature. M87: Biretta, Stern & Harris (1991), Despringre, Fraix-Burnet & Davoust (1996), Tan et al. (2008), Perlman et al. (2001), Balmaverde, Capetti & Grandi (2006), Ackermann et al. (2015), Broderick et al. (2015), Aharonian et al. (2006), Aliu et al. (2012). Cen A: Meisenheimer et al. (2007), Grandi et al. (2003), Harmon et al. (2004), Ackermann et al. (2015), Aharonian et al. (2009). The Compton Gamma Ray Observatory fluxes of Cen A, collected during a multi-frequency campaign in 1995, are provided by H. Steinle on the web page http://www.mpe.mpg.de/ hcs/Cen-A/ and included in NED.

shift in the SED due to the relativistic beaming, but also to differences in the emitting regions. Indeed, due to the presence of a velocity stratification with the relativistic jets (Kovalev et al. 2007; Nagai et al. 2014) in BL Lacs, we are seeing the regions of the jet with the highest Doppler factor (the so-called jet spine) while in FR Is, the emission could be dominated by the slower jet layers. The SED differences might be due to the diverse physical conditions in these two regions (Chiaberge et al. 2000; Ghisellini et al. 2005; Tavecchio & Ghisellini 2014), leading to a dependence of their shape on the viewing angle.

This effect might account for the SED differences between M87 and Tol1326−379 and, on the other hand, the similarities with Centaurus A. Indeed, the M87 jet is seen at a rather small angle from the line of sight with $\theta \sim 15$–25° (Acciari et al. 2009), while Cen A lies close to the plane of the sky, $\theta \sim 50$–80° (Tingay et al. 1998). We argue that the SED shapes, as derived from the comparison between BL Lacs and FR Is, are mainly driven by the jet viewing angle. Indeed, by excluding Centaurus A, all the FR Is have flat γ-ray spectra and are seen at small angles (see Table 1). The only exception is 3C 120, which has a slope comparable to that of Cen A (and Tol1326−379), but a smaller inclination angle. 3C 120 is, however, a peculiar RG. Although classified as an FR I, it has optical-UV-X-ray properties typical of FR IIs. It shows broad optical emission lines (Tadhunter et al. 1993), an UV bump and a K α iron line in the X-ray spectrum (Zdziarski & Grandi 2001; Ogle et al. 2005; Kataoka et al. 2007; Chatterjee et al. 2011), all clear signatures of the presence of an efficient accretion disc. Indeed, in Fig. 4 (right-hand panel), 3C 120 falls between 3C 111 ($\Gamma = 2.79$, $L_\gamma = 43.21$) and Pictor A ($\Gamma = 2.49$, $L_\gamma = 42.65$), two (FR II) BLRGs detected by *Fermi*.

Although we do not have any direct estimate for the orientation of Tol1326−379, we speculate that it is oriented at a large angle and this causes the similarity between its SED and that of Cen A.

Table 1. Jet inclination angle from the literature, γ-ray spectral slope (Γ) and luminosity L_γ [>1 GeV] (erg s^{-1}) of the FR I RGs.

Source	θ	Γ	L_γ	Ref.
3C 78	50°	2.07 ± 0.11	42.92	1
IC 310	<20°	1.90 ± 0.14	42.70	2
NGC 1275	30–55°	1.95 ± 0.01	44.03	3
B20331+39	<45°	2.11 ± 0.17	42.40	4
3C 120[a]	18–22°	2.7 ± 0.1	42.75	5
PKS 0625−45	<61°	1.87 ± 0.05	44.00	6
3C 189	27°	2.16 ± 0.16	42.86	7
3C 264	∼50°	1.98 ± 0.19	42.37	8
M87	15–25°	2.05 ± 0.06	41.61	9
Cen A	50–80°	2.70 ± 0.03	41.00	10
Cen B[a, b]	<80°	2.32 ± 0.09	42.63	11
NGC 6251	10–40°	2.04 ± 0.08	42.87	12

Notes. [a]Cen B and 3C 120 are not in the clean 3LAC sample.
[b]Cen B: Jet inclination upper limit estimated using the jet/counterjet flux ratio $J \sim 2$ at 4.8 GHz provided by Jones, Lloyd & McAdam (2001). Possible γ-ray contribution from the lobes (Katsuta et al. 2013).
(1) Kharb et al. (2009), (2) Schulz et al. (2015), (3) Walker, Romney & Benson (1994), (4) Giovannini et al. (2001), (5) Jorstad et al. (2005), (6) Venturi et al. (2000), (7) Bondi et al. (2000), (8) Lara et al. (2004), (9) Acciari et al. (2009), (10) Tingay et al. (1998), (11) Jones et al. (2001), (12) Migliori et al. (2011).

Alternatively, if we are seeing the jet of Tol1326−379 at a small angle, its SED would be intrinsically different from those of the FR Is. This would be the first indication of a discrepant property between these two classes (other than the paucity of extended radio emission for FR 0s) and might be an important clue in understanding their nature. Interestingly enough, the Compton peak for Tol1326−379 appears to be more prominent than the synchrotron one. This generally occurs for FSRQs, where a surplus of seed photons from the accretion disc, the broad-line region and the torus contributes to the high-energy emission by external Compton (Sikora et al. 2009). Incidentally, we note that Tol1326−379 is characterized by a steep γ-ray spectrum ($\Gamma_\gamma = 2.78 \pm 0.14$), more similar to that generally observed for FSRQs (and their misaligned population, i.e. BLRGs and SSRQs) than for BL Lacs (and FR Is). It is, however, improbable that an external Compton mechanism is responsible for cooling the jet particles of Tol1326−379. Its nuclear environment is poor in photons as indicated by the low accretion rate. It is then more plausible that its γ-ray luminosity is sustained by different jet components that mutually interact, amplifying the IC emission as suggested for FR Is. The excess of γ-ray radiation could then reflect the different physical conditions of the high-energy dissipation regions (i.e. of the spine and/or the layers).

Progress in our understanding of the properties of Tol1326−379 can come from a better definition of its SED. In particular, the information in the X-rays could be improved with a firm detection and with a measurement of the spectral slope in this band. This might be used to test the indication that the Compton peak in Tol1326−379 is more prominent than the synchrotron one.

Since a large diversity of spectral behaviour among this class of sources, as already observed in blazars, cannot be excluded, other observations of γ-rays emitting FR 0s are necessary to consolidate the overall picture.

ACKNOWLEDGEMENTS

We are grateful to F. Paresce for carefully reading the paper and useful comments, which improved the final version. We thank the referee for constructive comments and suggestions on the manuscript. This research made use of the NASA/IPAC Infrared Science Archive and Extragalactic Database, which is operated by the Jet Propulsion Laboratory, California Institute of Technology, under contract with the National Aeronautics and Space Administration. Part of this work is based on archival data, software or online services provided by the Scientific Data Center of the Italian Space Agency.

REFERENCES

Abdo A. A. et al., 2010a, ApJS, 188, 405
Abdo A. A. et al., 2010b, Science, 328, 725
Abdo A. A. et al., 2010c, ApJ, 720, 912
Acciari V. A. et al., 2009, Science, 325, 444
Acero F. et al., 2015, ApJS, 218, 23
Ackermann M. et al., 2011, ApJ, 741, 30
Ackermann M. et al., 2015, ApJ, 810, 14
Aharonian F. et al., 2006, Science, 314, 1424
Aharonian F. et al., 2009, ApJ, 695, L40
Aliu E. et al., 2012, ApJ, 746, 141
Baldi R. D., Capetti A., 2009, A&A, 508, 603
Baldi R. D., Capetti A., 2010, A&A, 519, A48
Baldi R. D., Capetti A., Giovannini G., 2015a, A&A, 576, A38
Baldi R. D., Capetti A., Giovannini G., 2015b, 5th Workshop on CSS and GPS radio sources, Astronomische Nachrichten, in press, preprint (arXiv:1510.04272)
Balmaverde B., Capetti A., 2006, A&A, 447, 97
Balmaverde B., Capetti A., Grandi P., 2006, A&A, 451, 35
Balmaverde B., Baldi R. D., Capetti A., 2008, A&A, 486, 119
Becker J. K., Biermann P. L., 2009, Astropart. Phys., 31, 138
Best P. N., Heckman T. M., 2012, MNRAS, 421, 1569
Biretta J. A., Stern C. P., Harris D. E., 1991, AJ, 101, 1632
Bondi M., Parma P., de Ruiter H., Fanti R., Laing R. A., Fomalont E. B., 2000, MNRAS, 314, 11
Böttcher M., 2012, Fermi & Jansky Proceedings, eConf C1111101, preprint (arXiv:1205.0539)
Böttcher M., Dermer C. D., 2010, ApJ, 711, 445
Broderick A. E., Narayan R., Kormendy J., Perlman E. S., Rieke M. J., Doeleman S. S., 2015, ApJ, 805, 179
Buttiglione S., Capetti A., Celotti A., Axon D. J., Chiaberge M., Macchetto F. D., Sparks W. B., 2010, A&A, 509, A6
Casadio C. et al., 2015, ApJ, 808, 162
Chatterjee R. et al., 2011, ApJ, 734, 43
Chiaberge M., Marconi A., 2011, MNRAS, 416, 917
Chiaberge M., Celotti A., Capetti A., Ghisellini G., 2000, A&A, 358, 104
Condon J. J., Cotton W. D., Greisen E. W., Yin Q. F., Perley R. A., Taylor G. B., Broderick J. J., 1998, AJ, 115, 1693
Despringre V., Fraix-Burnet D., Davoust E., 1996, A&A, 309, 375
Fabbiano G., Kim D.-W., Trinchieri G., 1992, ApJS, 80, 531
Fanaroff B. L., Riley J. M., 1974, MNRAS, 167, 31P
Feain I. J. et al., 2009, ApJ, 707, 114
Georganopoulos M., Kazanas D., 2003, ApJ, 589, L5
Ghirlanda G., Ghisellini G., Tavecchio F., Foschini L., 2010, MNRAS, 407, 791
Ghisellini G., Tavecchio F., Chiaberge M., 2005, A&A, 432, 401
Giannios D., Uzdensky D. A., Begelman M. C., 2010, MNRAS, 402, 1649
Giovannini G., Cotton W. D., Feretti L., Lara L., Venturi T., 2001, ApJ, 552, 508
Grandi P. et al., 2003, ApJ, 593, 160
Grandi P., Torresi E., Stanghellini C., 2012, ApJ, 751, L3
Griffith M. R., Wright A. E., 1993, AJ, 105, 1666
Harmon B. A. et al., 2004, ApJS, 154, 585
Healey S. E., Romani R. W., Taylor G. B., Sadler E. M., Ricci R., Murphy T., Ulvestad J. S., Winn J. N., 2007, ApJS, 171, 61
Heckman T. M., Best P. N., 2014, ARA&A, 52, 589
Heckman T. M., Kauffmann G., Brinchmann J., Charlot S., Tremonti C., White S. D. M., 2004, ApJ, 613, 109

Jones P. A., Lloyd B. D., McAdam W. B., 2001, MNRAS, 325, 817
Jones D. H. et al., 2004, MNRAS, 355, 747
Jones D. H. et al., 2009, MNRAS, 399, 683
Jorstad S. G. et al., 2005, AJ, 130, 1418
Kataoka J. et al., 2007, PASJ, 59, 279
Katsuta J. et al., 2013, A&A, 550, A66
Kewley L. J., Groves B., Kauffmann G., Heckman T., 2006, MNRAS, 372, 961
Kharb P., Gabuzda D. C., O'Dea C. P., Shastri P., Baum S. A., 2009, ApJ, 694, 1485
Khiali B., de Gouveia Dal Pino E. M., Sol H., 2015, MNRAS, submitted preprint (arXiv:1504.07592)
Kovalev Y. Y., Lister M. L., Homan D. C., Kellermann K. I., 2007, ApJ, 668, L27
Lara L., Giovannini G., Cotton W. D., Feretti L., Venturi T., 2004, A&A, 415, 905
Mannucci F., Basile F., Poggianti B. M., Cimatti A., Daddi E., Pozzetti L., Vanzi L., 2001, MNRAS, 326, 745
Marconi A., Hunt L. K., 2003, ApJ, 589, L21
Massaro F., D'Abrusco R., Ajello M., Grindlay J. E., Smith H. A., 2011, ApJ, 740, L48
Mauch T., Murphy T., Buttery H. J., Curran J., Hunstead R. W., Piestrzynski B., Robertson J. G., Sadler E. M., 2003, MNRAS, 342, 1117
Meisenheimer K. et al., 2007, A&A, 471, 453
Migliori G. et al., 2011, A&A, 533, A72
Murphy T. et al., 2010, MNRAS, 402, 2403
Nagai H. et al., 2014, ApJ, 785, 53
Ogle P. M., Davis S. W., Antonucci R. R. J., Colbert J. W., Malkan M. A., Page M. J., Sasseen T. P., Tornikoski M., 2005, ApJ, 618, 139
Perlman E. S., Sparks W. B., Radomski J., Packham C., Fisher R. S., Piña R., Biretta J. A., 2001, ApJ, 561, L51
Sadler E. M., Ekers R. D., Mahony E. K., Mauch T., Murphy T., 2014, MNRAS, 438, 796
Schulz R. et al., 2015, 12th European VLBI Network Symposium and Users Meeting EVN 2014. Cagliari, Italy, preprint (arXiv:1502.03559)
Shaw M. S. et al., 2012, ApJ, 748, 49
Sikora M., Stawarz Ł., Moderski R., Nalewajko K., Madejski G. M., 2009, ApJ, 704, 38
Stickel M., Fried J. W., Kuehr H., Padovani P., Urry C. M., 1991, ApJ, 374, 431
Tadhunter C. N., Morganti R., di Serego-Alighieri S., Fosbury R. A. E., Danziger I. J., 1993, MNRAS, 263, 999
Tan J. C., Beuther H., Walter F., Blackman E. G., 2008, ApJ, 689, 775
Tavecchio F., Ghisellini G., 2014, MNRAS, 443, 1224
Tingay S. J. et al., 1998, AJ, 115, 960
Urry C. M., Padovani P., 1995, PASP, 107, 803
Venturi T., Morganti R., Tzioumis T., Reynolds J., 2000, A&A, 363, 84
Walker R. C., Romney J. D., Benson J. M., 1994, ApJ, 430, L45
Whittle M., 1985, MNRAS, 213, 33
Wright A. E., Griffith M. R., Burke B. F., Ekers R. D., 1994, ApJS, 91, 111
Wright E. L. et al., 2010, AJ, 140, 1868
Zdziarski A. A., Grandi P., 2001, ApJ, 551, 186

This paper has been typeset from a TEX/LATEX file prepared by the author.